Global Biogeochemical Cycles

RESEARCH ARTICLE
10.1029/2025GB008832

Inundation and Sediment Supply Predict Annual but Not Centennial Carbon Accumulation in Tidal Wetlands Across Land-Use Types

Katrina L. Poppe[1,2], John M. Rybczyk[1], Christopher N. Janousek[3], Scott D. Bridgham[4], Craig Cornu[5], Trevor Williams[3], Heida L. Diefenderfer[6,7], Amy B. Borde[8], Heather Perillat[4], Laura S. Brophy[5], Erin K. Peck[9], Jude Apple[10], and Sara H. Knox[2,11]

[1]Western Washington University, Bellingham, WA, USA, [2]University of British Columbia, Vancouver, BC, Canada, [3]Oregon State University, Corvallis, OR, USA, [4]University of Oregon, Eugene, OR, USA, [5]Institute for Applied Ecology, Corvallis, OR, USA, [6]Pacific Northwest National Laboratory, Sequim, WA, USA, [7]University of Washington, Seattle, WA, USA, [8]Columbia Land Trust, Vancouver, WA, USA, [9]University of Rhode Island, Kingston, RI, USA, [10]Padilla Bay National Estuarine Research Reserve, Mt Vernon, WA, USA, [11]McGill University, Montreal, QC, Canada

Key Points:

- Contemporary inundation frequency and sediment load were good predictors of short-term, but not long-term, carbon accumulation rates
- Diking suppresses carbon accumulation rates, but tidal reconnection quickly reverses this effect
- Elevation change rates calibrated to accretion rates enabled accretion estimates at disturbed sites, where conventional methods often fail

Supporting Information:

Supporting Information may be found in the online version of this article.

Correspondence to:

K. L. Poppe,
poppek@student.ubc.ca

Citation:

Poppe, K. L., Rybczyk, J. M., Janousek, C. N., Bridgham, S. D., Cornu, C., Williams, T., et al. (2026). Inundation and sediment supply predict annual but not centennial carbon accumulation in tidal wetlands across land-use types. *Global Biogeochemical Cycles*, *40*, e2025GB008832. https://doi.org/10.1029/2025GB008832

Received 14 AUG 2025
Accepted 7 JUN 2026

Author Contributions:

Conceptualization: Katrina L. Poppe, John M. Rybczyk, Christopher N. Janousek, Scott D. Bridgham, Craig Cornu, Heida L. Diefenderfer, Amy B. Borde, Laura S. Brophy, Jude Apple
Data curation: Katrina L. Poppe, Christopher N. Janousek
Formal analysis: Katrina L. Poppe, Erin K. Peck
Funding acquisition: Katrina L. Poppe, John M. Rybczyk, Christopher N. Janousek, Scott D. Bridgham, Craig Cornu, Heida L. Diefenderfer, Amy B. Borde, Laura S. Brophy, Jude Apple, Sara H. Knox

Abstract Despite growing interest in the contributions of tidal wetlands to natural climate solutions, data remain scarce on how land use affects their carbon accumulation rates (CAR). Additionally, environmental factors driving the large observed variability in CAR among sites are poorly understood. To address these knowledge gaps, we measured short-term (~1 year) and long-term (~100 years) CAR using feldspar marker horizons, ^{210}Pb profiles, and surface elevation tables from 39 sites in seven estuaries in Oregon and Washington, USA. Sites varied in wetland type (tidal marsh, tidal swamp, nontidal pasture), land-use history (reference, restored, and disturbed), and salinity (fresh to polyhaline). Across both timescales, CAR was lowest in disturbed pastures and highest in restored marshes, reflecting patterns in sediment accretion rates. Short-term CAR exceeded long-term CAR by approximately 50% on average and was only weakly correlated with long-term CAR, with differences among hydrogeomorphic setting. Short-term CAR was well predicted by summer inundation frequency and relative sediment load, together explaining 60% of variance, whereas long-term CAR was poorly predicted by contemporary environmental conditions. These findings highlight the importance of aligning predictor and response timescales when modeling blue carbon dynamics, and reinforce the climate mitigation potential of tidal wetland restoration.

Plain Language Summary Tidal wetlands help mitigate climate change by storing carbon in their soils. However, we still lack information on how different land uses and local environmental conditions influence how quickly this carbon is buried. We measured both short-term (about 1 year) and long-term (about 100 years) carbon accumulation rates at 39 wetland sites in Oregon and Washington, USA, including natural, restored, and disturbed areas. Short-term carbon accumulation was higher than long-term accumulation and was more closely linked to present-day flooding and sediment supply. Carbon accumulation was lowest in disturbed wetlands with restricted tidal flow and higher in restored marshes, showing that restoring tidal wetlands can rapidly boost carbon accumulation by enhancing sediment build-up.

1. Introduction

Tidal wetlands exhibit high rates of soil carbon accumulation, roughly an order of magnitude greater than terrestrial ecosystems, due to high rates of primary production, anaerobic soil conditions that slow organic matter decomposition, and high sediment delivery through tidal inundation leading to carbon burial (Chmura et al., 2003; McLeod et al., 2011). Carbon accumulation rates (CAR) derived from dated soil cores can provide a long-term estimate of the belowground portion of net ecosystem carbon balance (NECB). NECB represents the net rate of carbon accumulation by an ecosystem as a result of both vertical and lateral carbon fluxes (Chapin et al., 2006, 2011), and it is an important component of greenhouse gas inventories (Holmquist et al., 2018). Despite the increasing study of CAR in tidal wetlands in recent years, there are comparatively few CAR estimates available from disturbed tidal wetlands that have been diked and converted to agricultural use. Here, disturbance refers specifically to hydrologic alteration that reduces tidal exchange. This imbalance in data availability may reflect the difficulty of applying conventional soil dating methods in disturbed soils (Arias-Ortiz et al., 2018), and limits

Investigation: Katrina L. Poppe, John M. Rybczyk, Christopher N. Janousek, Scott D. Bridgham, Craig Cornu, Trevor Williams, Amy B. Borde, Heather Perillat
Methodology: Katrina L. Poppe, John M. Rybczyk, Christopher N. Janousek, Scott D. Bridgham, Craig Cornu, Trevor Williams, Heida L. Diefenderfer, Amy B. Borde, Laura S. Brophy, Erin K. Peck, Jude Apple, Sara H. Knox
Project administration: Christopher N. Janousek, Craig Cornu
Supervision: John M. Rybczyk, Christopher N. Janousek, Scott D. Bridgham, Sara H. Knox
Writing – original draft: Katrina L. Poppe
Writing – review & editing: Katrina L. Poppe, John M. Rybczyk, Christopher N. Janousek, Scott D. Bridgham, Craig Cornu, Trevor Williams, Heida L. Diefenderfer, Heather Perillat, Laura S. Brophy, Erin K. Peck, Sara H. Knox

our ability to predict the climate impact of land-use change in tidal wetlands (Crooks et al., 2020; Macreadie et al., 2021; Taillardat et al., 2020).

Within least-disturbed (reference) tidal wetlands, the ability to accurately predict CAR is also limited, because of high spatial variability and an incomplete understanding of relevant environmental drivers (Holmquist et al., 2018; Macreadie et al., 2019). Globally, CAR values span several orders of magnitude, particularly in mangroves and salt marshes (Breithaupt & Steinmuller, 2022; Wang et al., 2021). On a regional to global scale, the rate of relative sea-level rise (RSLR) has emerged as an important environmental predictor of CAR (Kirwan & Mudd, 2012; McTigue et al., 2019; Miller et al., 2022; Rogers et al., 2019; Wang et al., 2019, 2021). Additional predictors include latitude, tidal range, inundation frequency, elevation, and plant community composition (Adame et al., 2010; Chmura et al., 2003; Ouyang & Lee, 2014). However there remains much variability at local to regional scales, where other parameters tied to sediment availability appear to be influential such as estuarine sediment trapping efficiency (Peck et al., 2020), hydrologic connectivity and freshwater input (Breithaupt & Steinmuller, 2022; Fennessy et al., 2019), and distance to tidal channels (Chmura & Hung, 2004). Variability in CAR tends to parallel variability in sediment accretion rates more than soil carbon density (Chmura et al., 2003; Peck et al., 2020; Wollenberg et al., 2018), so the conditions that facilitate sediment accumulation in these environments must be considered in studies of CAR.

Consequently, assessing how environmental conditions and land-use change affect carbon sequestration requires more data from sites with a history of disturbance (i.e., diking that reduces tidal influence), and evaluation of predictors at relevant temporal and spatial scales. This study addresses this knowledge gap by quantifying both short-term (~1 year) and long-term (~100 years) CAR and measuring hypothesized environmental predictors at a diverse set of sites from multiple estuaries across the Pacific Northwest (PNW) region of the United States, representing a range of wetland types, land uses, and salinity regimes. Short-term CAR was included to align with the timescale of most environmental predictors, whereas long-term CAR is more commonly used in blue carbon accounting (IPCC, 2019).

Our main research questions were: (a) Does CAR differ by measurement timescale? (b) How does CAR vary among different wetland types and land-use histories in the PNW? and (c) What environmental factors best predict CAR variability across this diverse range of sites? We hypothesized that: (a) Short-term CAR would exceed long-term CAR, due to reduced compaction and decomposition over shorter timescales and changes in environmental conditions over the past century; (b) CAR would be lowest in disturbed former tidal wetlands and highest in restored marshes, consistent with patterns in sediment accretion associated with inundation; (c) Reference tidal marshes and swamps would have comparable CAR, with higher accretion rates in marshes offset by higher soil carbon density in swamps; and (d) Among the potential environmental predictors of CAR, hydrologic and sediment supply variables would be the most important, given the strong influence of sediment delivery in other reference tidal wetlands in the PNW (Peck et al., 2020). Because this study was conducted within a single climatic region, we expected variables associated with plant productivity and organic matter decomposition (e.g., temperature, salinity, and latitude) to be less influential.

2. Methods

2.1. Study Sites

We selected 39 sites across seven estuaries in Oregon and Washington to capture a range of tidal wetland types (emergent marsh, forested swamp, nontidal pasture), land-use history (reference, restored, disturbed), and salinity classes (freshwater, oligohaline, mesohaline, polyhaline; Figure 1 and Table S1 in Supporting Information S1). Reference wetlands included oligohaline to polyhaline emergent tidal marshes and freshwater to oligohaline forested tidal swamps (Table S1 in Supporting Information S1). Restored marshes were previously diked wetlands that had been reconnected to tidal influence 1–27 years prior to sampling, generally via dike breaching or dike removal. Marshes were mainly vegetated by perennial grasses, sedges, and forbs, while swamps were characterized by a Sitka spruce (*Picea sitchensis*) or red alder (*Alnus rubra*) overstory, with shrubs and herbaceous vegetation in the understory. Disturbed sites were mainly former tidal wetlands that had been diked to restrict tidal influence, and had become dominated by emergent graminoids, with some sites actively managed for agriculture and others where agriculture was abandoned sometime in the past. Disturbed sites were subdivided into "wet" and "dry" pastures, with wet pastures defined as having a median water table level within 25 cm of the surface for at least 5 months of the year (Williams et al., 2025). We use the term "wetland type" hereafter to refer

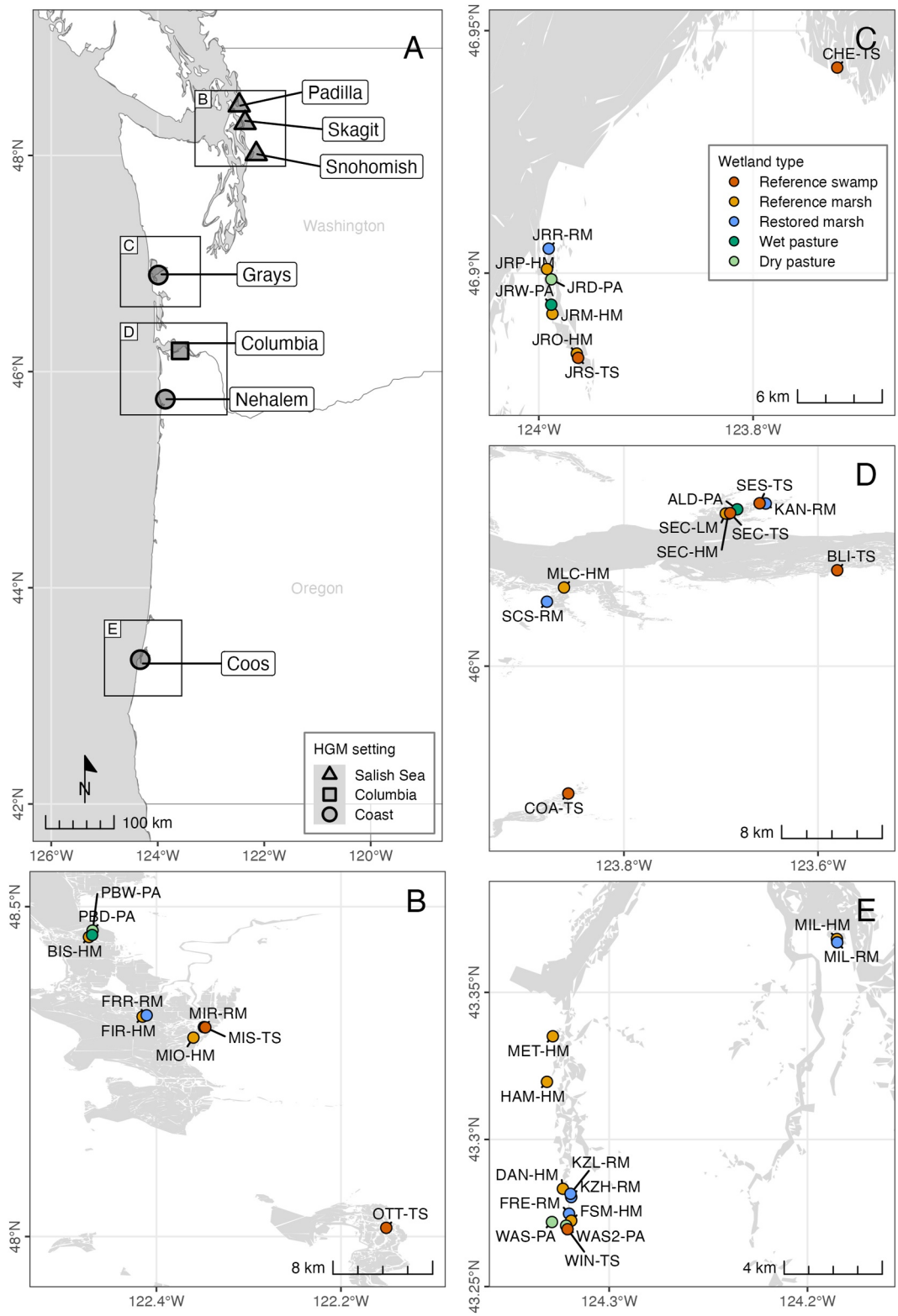

Figure 1. Location of 39 study sites in Washington and Oregon, USA. (a) Regional overview of study estuaries and associated hydrogeomorphic (HGM) setting. (b–e) Individual study sites and associated wetland types. Panels (b–e) use the Pacific Marine and Estuarine Fish Habitat Partnership's West Coast USA Estuarine Biotic Habitat map as basemap (Pacific Marine and Estuarine Fish Habitat Partnership, 2019).

to the five combinations of wetland types and land-use types: reference swamp, reference marsh, restored marsh, wet pasture, and dry pasture (Table S1 in Supporting Information S1).

2.2. Field Sampling

We collected two replicate sediment cores from each site to approximately 50 cm depth, targeting recovery of the full excess ^{210}Pb horizon. We used either PVC coring tubes with 10 cm diameter, or a stainless steel gouge auger with 6 cm diameter, both manually driven into the sediment. Recovered core lengths averaged 47.7 ± 7.8 cm (range 26.1–60.2 cm), with shorter recoveries occurring at disturbed and highly compacted sites. We measured core compaction by comparing the distance from the sediment surface to the top of the tube both inside and outside the PVC tube or the difference in sediment height at the open face of the gouge auger. Core compaction ranged from 0% to 17.8% across cores, and averaged 4.0 ± 4.2%.

We installed surface elevation tables (SETs) at select sites where the soil profile was expected to be disturbed and possibly not conducive to radiometric analysis (i.e., disturbed and restored land-use types; Lynch et al., 2015). We collected baseline measurements the same year as installation, then measured surface elevation once annually for three subsequent years. We used this 3-year time series to compute elevation change rates. We tracked pin height relative to initial pin height at each of nine pins and each of four arm positions (totaling 36 measurements per SET), then averaged across pins for each sampling event to regress mean elevation change against time. We use the slope of this regression as the SET elevation change rate.

We established 5–6 replicate 0.25 m^2 feldspar marker horizon plots at most sites to measure short-term sediment accretion, distributing them either randomly across the site or around SETs. We clipped aboveground plant biomass to the soil surface before installing the marker layer. Approximately 1 year later (0.8–1.4 years), we sampled each plot by removing two sediment wedges per plot with a knife, and measuring sediment thickness above the feldspar layer on up to four sides per wedge. We calculated accretion rates as sediment thickness divided by time since installation, averaging rates by wedge, plot, and site.

2.3. Environmental Predictor Measurements

We installed one 1.0–1.5 m deep PVC groundwater well at each site to measure water table level at 30-min intervals over approximately 1 year (Williams et al., 2025). We measured water table level with a Hobo U20 or U20L water-level sensor (Onset Corporation, Bourne, MA) suspended inside the well at a measured distance below ground. We measured conductivity and water temperature with an Odyssey logger (Dataflow Systems Ltd., Christchurch, NZ) suspended approximately 25 cm below the ground surface to reflect the root zone. We measured soil temperature at 1-hr intervals with Hobo pendant UA-001-08 loggers placed 5 cm below ground near each groundwater well. We periodically field verified logger salinity and temperature measurements with a YSI Pro30 conductivity probe. In some freshwater sites we only measured salinity with YSI probes during site visits, totaling 5–10 measurements throughout the year, because of limited temporal change in salinity. We estimated inundation frequency as the percentage of 30-min water table level measurements above the soil surface. For this and all other time series variables, we calculated annual and seasonal means by first computing day-of-year (DOY) means, then averaging across DOYs for the relevant time period, to ensure equal DOY weighting when time series spanned more than one full year.

We measured elevation at each core location with real-time kinematic global navigation satellite system (RTK-GNSS) with Trimble R8 and R12 (Trimble, Inc., Westminster, CO) and Eos Positioning Systems (Terrebonne QC, Canada) rovers. For forested sites, we used laser leveling from nearby benchmarks measured with RTK-GNSS. We converted these geodetic elevations in the North American Vertical Datum of 1988 (NAVD88) to tidal elevations with the formula $z^* = (z\text{-MTL})/(\text{MHHW-MTL})$, where z is the measured NAVD88 elevation, and mean tide level (MTL) and mean higher high water (MHHW) are local tidal datums in NAVD88 (Swanson et al., 2014). We obtained tidal datums from nearby NOAA tide gauge data (tidesandcurrents.noaa.gov), by computing datums from tidal channel water level time series (Janousek & Cornu, 2025; Janousek, Cornu, & Williams, 2025) following methods in NOAA (2003), and by estimating datums as needed using VDATUM 3.6.1 and 4.1.2 for MTL (https://vdatum.noaa.gov/). Channel water level loggers were maintained either by the authors or by the National Estuarine Research Reserve System (https://cdmo.baruch.sc.edu/).

Table 1
List of Estuary-Level Attributes Including Hydrogeomorphic (HGM) Setting, Rate of Relative Sea-Level Rise (RSLR), Watershed Area, Tidal Wetland Area, and Sediment Loads

Estuary	HGM setting	N sites	RSLR (cm y^{-1})	RSLR period of record	Watershed area (km^2)	Tidal wetland area (km^2)	Sediment load: Total (sed_{tot}) ($\times 10^3$ t yr^{-1})	Sediment load: Per wetland area (sed_{wet}) ($\times 10^3$ t yr^{-1} km^{-2})
Coos (OR)	Coast	13	0.110	1970–2023	1,556	8.2	207.8	25.3
Nehalem (OR)	Coast	1	0.252	1970–2023	2,209	2.6	632.7	274.4
Columbia (OR, WA)								
Columbia main river (OR, WA)	Columbia	3	0.025[a]	1926–2014	622,040	105.6	5255.1	49.7
Lewis and Clark (OR)	Columbia	2	0.025[a]	1926–2014	162	1.3	24.9	18.8
Grays River (WA)	Columbia	3	0.025[a]	1926–2014	322	4.0	61.2	15.2
Grays Harbor (WA)								
Johns River (WA)	Coast	7	0.043	1973–2023	81	2.4	6.8	2.8
Chehalis (WA)	Coast	1	0.043	1973–2023	5,490	37.0	648.0	17.5
Snohomish (WA)	Salish Sea	1	0.233	1920–2023	4,529	6.4	1182.4	186.3
Skagit (WA)	Salish Sea	5	0.182	1972–2023	8,061	16.3	4367.8	268.3
Padilla (WA)	Salish Sea	3	0.119	1934–2023	12	0.2	3.5	18.8

Note. We considered some Columbia River Estuary and Grays Harbor Estuary sites to be primarily influenced by tributaries to the main watershed. [a]RSLR rates from Talke et al. (2020) are discharge-corrected and datum-corrected.

We classified each study estuary into one of three hydrogeomorphic settings: (a) Columbia, which includes estuaries located within the larger Columbia River Estuary in Oregon and Washington, (b) Salish Sea, including estuaries located within the Salish Sea in Washington, and (c) Coast, which includes all other smaller estuaries along the outer Pacific coastline (Figure 1 and Table 1). This classification distinguishes large, river-dominated (Columbia), semi-enclosed marine (Salish Sea), and smaller, open-coast estuaries (Coast), which vary in freshwater input, tidal dynamics, exposure, and sediment supply. We grouped estuaries by hydrogeomorphic setting to provide an ecologically meaningful regional grouping for assessing CAR variability, alongside site and estuary scales.

We determined the rate of RSLR as the rate since 1920 from NOAA sea level trends (https://tidesandcurrents.noaa.gov/sltrends/) from the nearest tide gauge station (Table 1). We used this time period to correspond with the approximate 100-year timeframe represented by ^{210}Pb accretion rates. Many stations had a shorter period of record (often closer to 50 years), in which case we used the entire available period of record. For Columbia River Estuary sites, we used a discharge-corrected and datum-corrected RSLR rate from Talke et al. (2020).

We determined estuary-scale sediment loads and suspended sediment concentrations (SSC) with the USGS SPAtially-Referenced Regression on Watershed attributes (SPARROW) model (https://usgs.gov/tools/sparrow), identifying the watershed most relevant to the dominant sediment source for each site, which in some cases was a sub-watershed. We delineated estuary boundaries with the Pacific Marine and Estuarine Fish Habitat Partnership mapping data, using the West Coast USA Estuarine Biotic Habitat data layer downloaded into a geographic information system (Brophy et al., 2019; https://pacificfishhabitat.org/data/estuarine-biotic-habitat). From these delineations, we calculated total estuary area and vegetated estuary area. For total estuary area we included all tidal wetlands (tidal marsh, tidal scrub-shrub, and tidal forest), aquatic vegetation bed, eelgrass, benthic, and faunal bed habitats, and excluded non-tidal terrestrial habitats. Vegetated estuary area was a subset that included just intertidal wetlands (tidal marsh, tidal scrub-shrub, and tidal forest). We then derived two normalized sediment load metrics from the total sediment load (sed_{tot}): sediment load divided by total estuary area (sed_{est}), and sediment load divided by tidal wetland area (sed_{wet}; Table 1).

2.4. Sediment Analyses

We processed sediment cores by slicing them at 2-cm intervals, oven-drying at 60°C to a constant weight, and weighing them to determine bulk density based on sample volume. We ground samples with a mortar and pestle to pass through a 0.5 mm mesh sieve. We analyzed subsamples for organic matter content by loss-on-ignition at 550°C for approximately 8 hr (Heiri et al., 2001). We corrected for compaction by applying the compaction fraction evenly across each 2-cm core section, adjusting the reported top and bottom depths accordingly (for example, each 2-cm section from a core that experienced 1% compaction was adjusted to become a 2.02-cm section.

We estimated soil organic C (C_{org}) content by applying an established model of the relationship between organic matter content and carbon content for each soil sample. This OM-C_{org} model was developed for the U.S. West Coast and includes separate formulas according to wetland type, ecoregion, and organic matter content (Janousek, Krause, et al., 2025; Table S2 in Supporting Information S1).

For long-term sediment accretion rates, we measured ^{210}Pb activity with GL2820R and BE3825 germanium detectors (Mirion Technologies Inc., Meriden, CT) at Western Washington University. We calculated excess ^{210}Pb ($^{210}Pb_{xs}$) gamma emissions for each sample as the difference between total and supported ^{210}Pb emissions, recorded at 46 and 351 keV, respectively (Figure S1 in Supporting Information S1). We used the constant initial concentration model to determine the accretion rate based on the linear regression of the natural log of $^{210}Pb_{xs}$ against depth, where the accretion rate is equal to $-\lambda/s$, λ is the ^{210}Pb decay constant (0.03114 yr^{-1}), and s is the slope of the regression (Robbins et al., 1978; Figure S2 in Supporting Information S1). We limited this regression to the portion of the $^{210}Pb_{xs}$ profile with decreasing values, excluding any obvious mixed layer at the surface and eliminating deeper layers where $^{210}Pb_{xs}$ approached zero. We eliminated cores where the $^{210}Pb_{xs}$ profile indicated non-steady state accumulation or excessive mixing throughout. Some cores required case-specific interval selection decisions; core-specific explanations are provided in Table S3 of Supporting Information S1. For restored marsh cores, we limited the ^{210}Pb-based accretion rate to the portion of the $^{210}Pb_{xs}$ profile above any obvious restoration layer when possible, based on bulk density, organic matter content, and/or ^{210}Pb stratigraphy, to represent the post-restoration accretion rate (Drexler et al., 2019).

As expected, some cores at disturbed and restored sites showed evidence of soil disturbance that prevented us from determining accretion rates from the ^{210}Pb profile. We therefore used adjusted SET rates to approximate the timescale of the ^{210}Pb-derived accretion rates for these sites (Table S4 in Supporting Information S1). Other studies have used elevation change from SETs as a direct replacement for ^{210}Pb-derived accretion rates (e.g., Wang et al., 2021), but we have found SET rates to be consistently higher than ^{210}Pb rates in the PNW (Poppe & Rybczyk, 2021). Thus, for those sites where we could not interpret ^{210}Pb rates and had installed SETs, we estimated long-term accretion rates based on a linear relationship between SET elevation change rates and successfully dated ^{210}Pb accretion rates (^{210}Pb rate = 0.23*SET rate + 0.17, $R^2 = 0.73$, $p < 0.001$, $n = 19$; Figure S3 in Supporting Information S1). This regression included only cores that yielded interpretable ^{210}Pb accretion rates. To increase sample size for the purpose of this model, we included observations both from this study and a previous study in the Stillaguamish Estuary (Poppe & Rybczyk, 2021).

We calculated soil organic carbon density for each core increment as the product of bulk density and modeled organic carbon content. For short-term (i.e., feldspar) CAR estimates, we used carbon density from the surface (0–2 cm) depth interval. For long-term estimates, we averaged carbon density over the depth interval used to calculate the ^{210}Pb accretion rate. In cases where ^{210}Pb profiles were too mixed to permit reliable accretion estimates, we used a 100-year depth estimated from the SET-corrected accretion rate (rate × 100 years), since this aligns with the approximate timescale of the ^{210}Pb accretion rate (Robbins et al., 1978); for restored sites, the integration period was limited to years since restoration. We calculated CAR for each core as the product of mean carbon density and the ^{210}Pb-based accretion rate. We obtained 28 short-term CAR measurements from 28 sites, and 59 long-term CAR measurements from 39 sites (Table S4 in Supporting Information S1). We used the SET-^{210}Pb rate conversion for 8 sites (Table S4 in Supporting Information S1).

2.5. Statistical Analyses

We performed all analyses on site-level values with R Statistical Software (v4.5.2; R Core Team, 2025). We evaluated differences in CAR among wetland types and land-use types with nonparametric tests due to small and

unequal sample sizes across groups, although CAR itself was approximately normally distributed. We assessed non-directional differences among wetland types and land-use types using two-tailed Kruskal-Wallis tests, followed by Wilcoxon rank-sum post hoc tests, both within the rstatix R package (Kassambara, 2025). We also evaluated planned, directional contrasts among land-use types with exact permutation tests in the coin R package (Hothorn et al., 2006), based on a priori expectations that CAR would be relatively low in disturbed sites. We report effect sizes for these directional contrasts as rank-biserial correlation coefficients (r), from Wilcoxon effect size estimates. We assessed linear relationships between individual environmental predictors and CAR with Pearson correlations.

We used two complementary modeling approaches to identify the major predictors of CAR: linear mixed effects (LME) modeling and conditional inference trees (CITs). LME models can include both fixed and random effects to account for grouped observations such as sites within estuaries, but have parametric model assumptions. CITs do not accommodate random effects, but they are non-parametric and thus more flexible in their ability to identify non-linear relationships and interactions. CITs recursively partition data based on statistically significant relationships, using hypothesis testing to select splits and avoid bias from variable selection. We included CIT as a verification of the LME variable selection. We built two separate sets of models, one for short-term CAR, and one for long-term CAR. The short-term timescale (~1 year) most closely matches the measurement timescale of many environmental predictors, enabling interpretation of mechanistic relationships. Long-term CAR (~100 years) was modeled to explore whether contemporary predictors could explain centennial-scale CAR patterns, despite the inherent timescale mismatch. We considered the following predictor variables: tidal elevation (z*), water table level, inundation frequency, salinity, water temperature, soil temperature, RSLR, watershed size, sediment load, and latitude. For the soil and hydrological variables we included mean annual, mean summer (DOY >151 and DOY <244), and mean growing season (DOY >59 and DOY <244) values for consideration. For sediment load we considered total sediment load (sed_{tot}), sediment load relative to estuary area (sed_{est}), sediment load relative to tidal wetland area (sed_{wet}), and SSC.

We used the lme4 R package for LME modeling (Bates et al., 2015). We selected a priori a limited set of LME candidate models representing alternative, ecologically plausible predictor combinations, rather than relying on automated variable selection procedures, to avoid model overfitting given the relatively small sample size ($n < 40$ sites). When multiple predictors represented the same underlying process (e.g., hydrologic metrics such as water table level, inundation frequency, or tidal elevation, and annual vs. seasonal summaries), we selected a single representative predictor from each group using Akaike's information criterion for small sample size (AIC_c) using the MuMIn R package (Bartoń, 2023), with a threshold of $\Delta AIC_c > 2$ to interpret differences in model support. We then compared candidate models, including with and without the random effect, again using AIC_c. We checked for collinearity among predictors with variance inflation factors (VIFs) from main-effects models, with VIF values <4 considered acceptable. We calculated partial R^2 using the rsq package in R (Zhang, 2024) to determine the unique contribution of each predictor. We standardized all continuous predictor variables (subtracting the mean and dividing by the standard deviation) to compare the importance of parameter coefficients in the LME models. We implemented CIT with the ctree function in the partykit R package (Hothorn & Zeileis, 2015), fitting a global model using all possible predictors, with the default mincriterion = 0.95 (i.e., a 0.05 significance level).

3. Results

3.1. CAR, Sediment Accretion, and Soil Carbon Density Values

Short term CAR varied substantially among sites, ranging from 32.3 to 454.0 g C m^{-2} yr^{-1}, with an overall mean (±SD) of 139.1 ± 109.3 g C m^{-2} yr^{-1} (Table S4 in Supporting Information S1). The highest rate occurred at a site restored less than 1 year prior to feldspar installation (FRR-RM). Short-term sediment accretion rates ranged between 0.08 and 4.82 cm yr^{-1} and averaged 0.67 ± 0.94 cm yr^{-1}. Soil organic carbon density was comparatively less variable, spanning 9.4–49.9 mg C cm^{-3}, with a mean of 29.7 ± 10.7 mg C cm^{-3}.

Across sites, long-term CAR ranged from −17.1 to 236.0 g C m^{-2} yr^{-1} and averaged 91.3 ± 52.2 g C m^{-2} yr^{-1} (Table S4 in Supporting Information S1). The single negative CAR value resulted from a SET-derived accretion rate, as only SETs are capable of measuring negative rates. This negative rate was measured at a dry agricultural site (PBD-PA) that was actively tilled and subsiding at the time of sampling. Long-term accretion rates varied

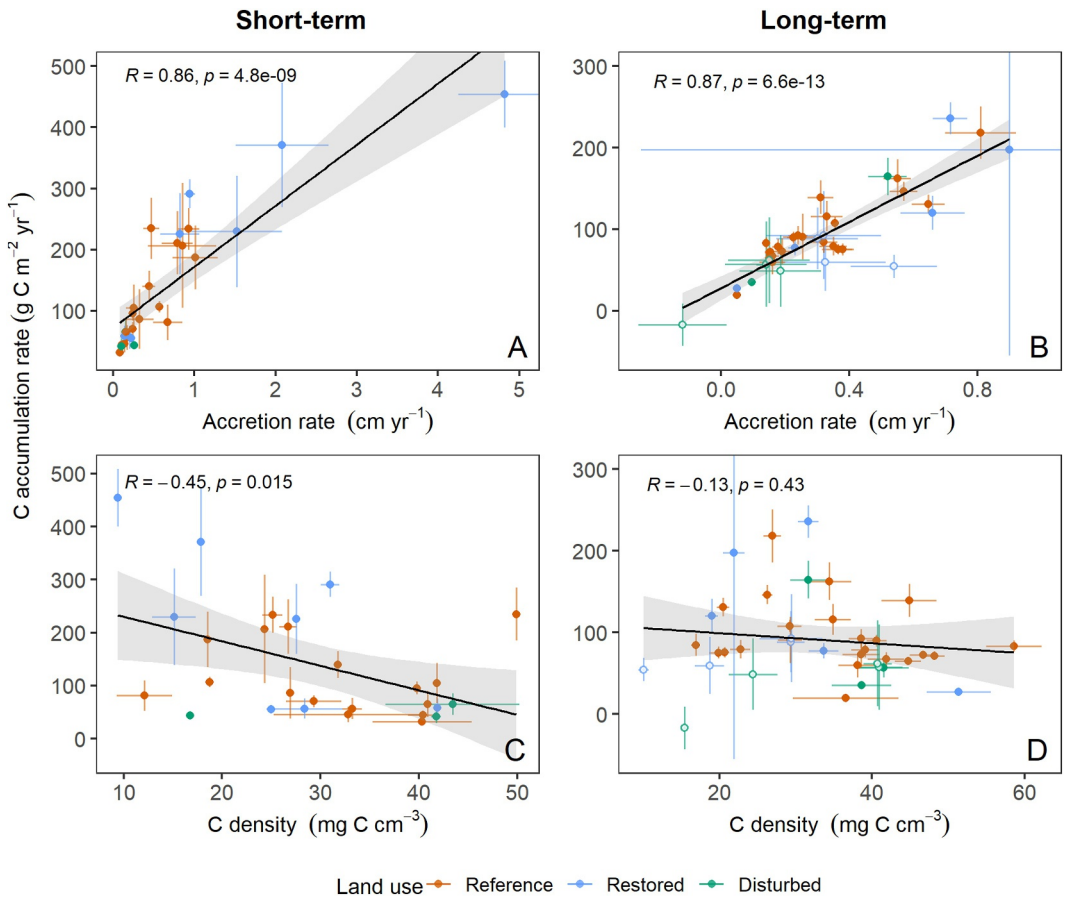

Figure 2. Site-level relationships between carbon accumulation rate (CAR) and accretion rate for (a) short-term and (b) long-term estimates, and between CAR and organic carbon density for (c) short-term and (d) long-term estimates. Hollow points in panels (b, d) indicate the use of adjusted SET rates to estimate long-term accretion. Error bars represent standard error. Gray bands are 95% confidence intervals around the linear regression lines.

from −0.12 to 0.90 cm yr^{-1} with a mean of 0.31 ± 0.22 cm yr^{-1}. Soil carbon density ranged from 10.1 to 58.6 mg C cm^{-3}, with a mean of 32.7 ± 11.0 mg C cm^{-3}.

Of the two variables in the CAR calculation, CAR was strongly positively correlated with accretion rate at both timescales (short-term: $r = 0.86$, $p < 0.001$; long-term: $r = 0.87$, $p < 0.001$; Figures 2a and 2b). In contrast, carbon density was negatively correlated with short-term CAR ($r = -0.45$, $p = 0.02$; Figure 2c), and was not significantly related to long-term CAR ($r = -0.13$, $p = 0.43$; Figure 2d). Accretion rate and carbon density were negatively correlated with each other (short-term: $r = -0.61$, $p < 0.001$; long-term: $r = -0.49$, $p = 0.001$; Figure S4 in Supporting Information S1).

3.2. Timescale Dependence of CAR

Paired comparisons revealed a timescale difference in CAR when all sites were considered together, with short-term CAR exceeding long-term CAR by approximately 50% overall ($p = 0.03$; Table S4 in Supporting Information S1). However, short- and long-term CAR were weakly correlated with each other across sites; while approximately half the sites showed comparable short- and long-term CAR values, many others had high short-term rates that did not scale proportionally to long-term rates (Figure 3). This results from differences in short- versus long-term accretion rates, because soil carbon density was greater in the long-term measurements ($p = 0.04$). When stratified by wetland type or land use, timescale differences in CAR were weaker (Tables S4 and S5 in Supporting Information S1). In contrast, grouping by HGM setting revealed a pronounced, consistent, and unique timescale difference in the Salish Sea, where short-term CAR was three times as high as long-term CAR ($p = 0.002$; Figure 3).

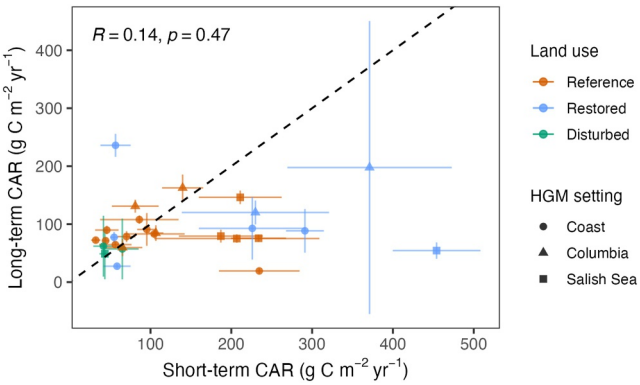

Figure 3. Relationship between short-term and long-term carbon accumulation rates (CAR) at the site level. Error bars indicate standard error. The dashed line represents a 1:1 relationship.

3.3. CAR Differences by Wetland Type and Land Use

Short-term CAR varied substantially within several wetland types (Figure 4), and non-directional tests did not detect differences among wetland types or land-use types (Tables S4 and S5 in Supporting Information S1). In contrast, planned directional tests consistent with a priori hypotheses indicated higher short-term CAR in reference than disturbed sites (p = 0.03, rank-biserial r = 0.46), and in restored than disturbed sites (p = 0.02, r = 0.55; Table S6 in Supporting Information S1). Differences between restored and reference sites were relatively modest but still supported statistically (p = 0.02, r = 0.28).

Long-term CAR likewise did not differ significantly among wetland types (Figure 4; Table S5 in Supporting Information S1). However, planned directional tests showed higher long-term CAR in reference than disturbed sites (p = 0.03, rank-biserial r = 0.47), with restored sites also tending to have higher long-term CAR than disturbed sites, although support was weaker (p = 0.08, r = 0.41; Table S6 in Supporting Information S1). Lastly, long-term CAR in restored sites was not detectably higher than in reference sites (p = 0.29, r = 0.004).

3.4. Environmental Predictors of CAR

Linear relationships between individual environmental predictor variables and CAR were generally stronger with short-term CAR than with long-term CAR, and in some cases changed sign (Figure 5). Among hydrologic variables, summer inundation frequency was the strongest correlate of short-term CAR, whereas summer water table level was the strongest—and only significant—correlate of long-term CAR. For short-term CAR, relative sediment load (sed_{wet}) was the strongest sediment-related correlate, while deep water temperature was the strongest temperature-related correlate, and tidal elevation (z*) was also significantly associated with CAR.

The strongest model of short-term CAR was a linear model with summer inundation frequency (β = 67.91, SE = 13.28, $p < 0.001$) and estuary-scale sediment load relative to tidal wetland area (sed_{wet}) (β = 51.76, SE = 13.28, p = 0.001) as fixed effects, explaining 60% of variance in CAR. Inundation frequency was the dominant predictor in the model, explaining more unique variance in short-term CAR (partial R^2 = 0.51) than relative sediment load (partial R^2 = 0.38). Sediment load helped distinguish some sites with relatively low inundation frequencies but high short-term CAR, indicating that sediment supply can partially offset lower flooding frequency (Figure 6). The random effect of estuary increased AIC_c by 3 units, indicating better support for the simpler linear (non-mixed) model. The model's predictive performance, assessed using leave-one-out-cross-validation, provided an R^2 of 0.54, suggesting good generalizability (Figure S5 in Supporting Information S1).

The strongest model of long-term CAR included only mean summer water table level as a fixed effect, with higher water table levels associated with higher CAR (β = 17.52, SE = 8.57, p = 0.05; Figure 6), and again no random effect. This model explained 9% of CAR variance, and had very low generalizability with a predicted versus observed R^2 of 0.01 (Figure S5 in Supporting Information S1).

The conditional inference tree for short-term CAR identified summer inundation frequency as the sole determinant of CAR (Figure S6 in Supporting Information S1). The split occurred at 6.42% (p = 0.02), with higher CAR values at higher inundation frequencies. This result was consistent with the linear model, which also identified summer inundation frequency as the most influential predictor of short-term CAR. In contrast, the CIT for long-term CAR did not identify any significant splits, indicating that none of the predictors were strongly associated with CAR at the 0.05 significance level, supporting the weak linear model performance for long-term CAR.

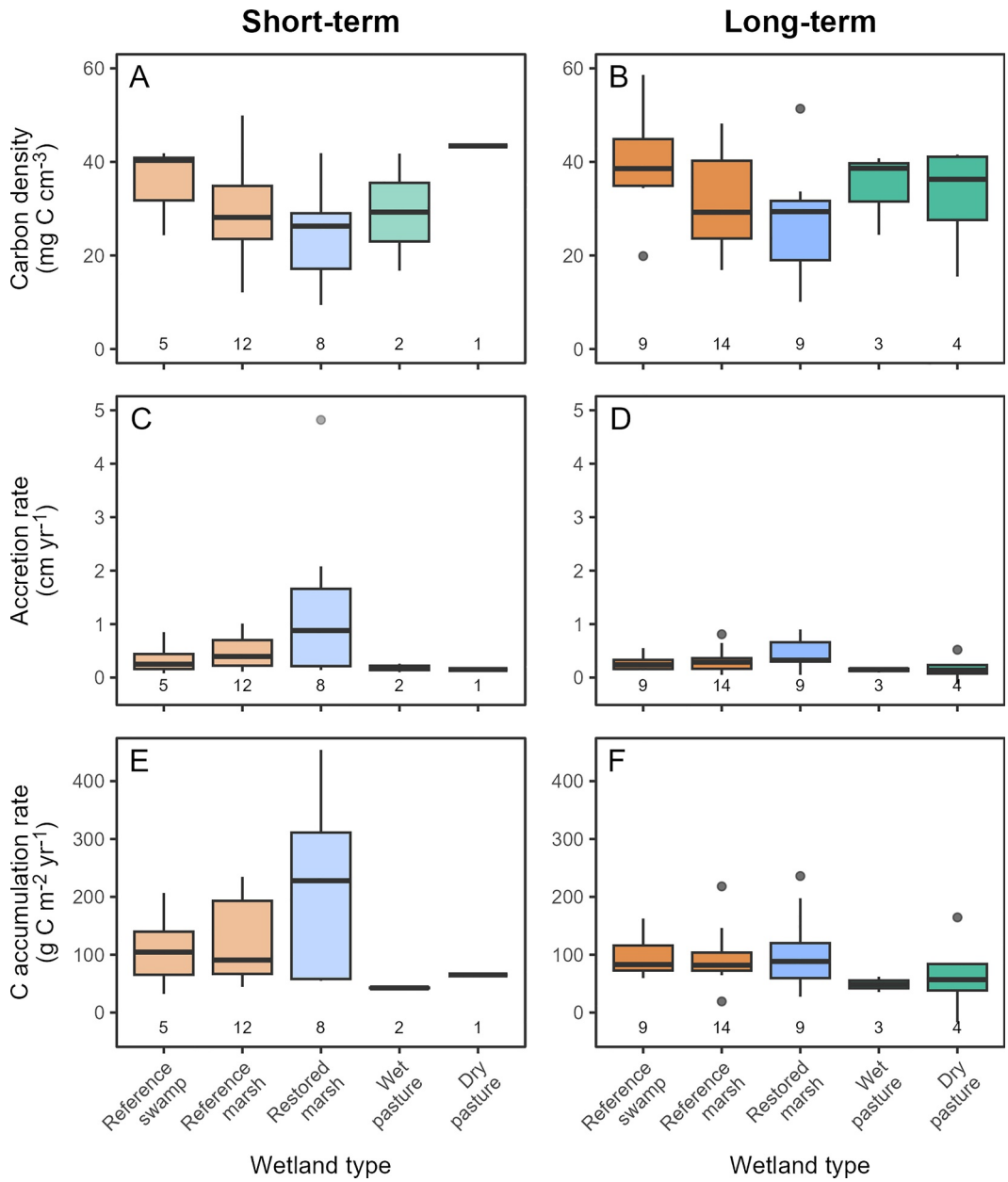

Figure 4. Distribution of soil carbon density (a, b), sediment accretion rate (c, d), and carbon accumulation rate (e, f) across five wetland types in the PNW. Short-term estimates are shown in the left column (a, c, e) and long-term estimates in the right column (b, d, f). Reference sites are colored orange, restored sites blue, and disturbed sites green. Boxplots show the median (horizontal lines), 25th and 75th percentiles (outer box edges), 5th and 95th percentiles (whiskers), and outliers (dots). Numbers below boxes indicate the number of sites.

4. Discussion

4.1. CAR Across Land Uses

Across both short- and long-term timescales, CAR values were consistently lower in disturbed sites than in reference wetlands, indicating that the hydrologic alteration associated with diking results in a lasting reduction in carbon accumulation. However, restored sites showed relatively high CAR, especially in the short-term, demonstrating that restoring tidal flow is effective in enhancing carbon accumulation. Notably, the restored sites in this study were relatively young at the time of sampling, yet they already showed CAR similar to or greater than that of reference wetlands over short timescales, suggesting that CAR responds very quickly to tidal reconnection.

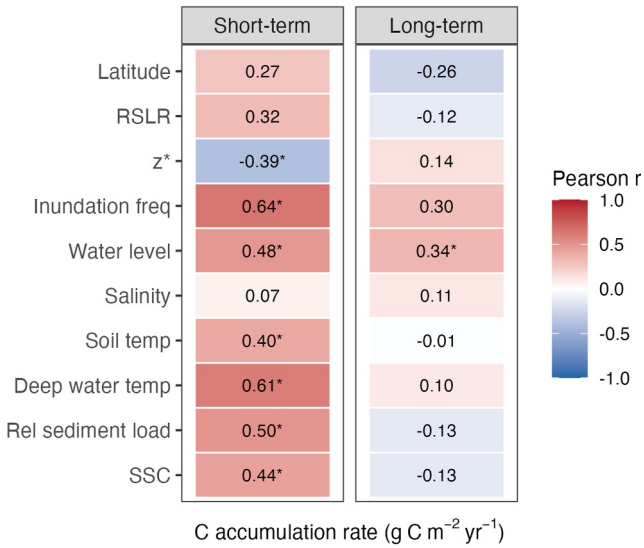

Figure 5. Pearson correlations between environmental predictor variables and short-term ($n = 28$) and long-term ($n = 39$) carbon accumulation rates. Asterisks indicate significant correlations ($p < 0.05$). Hydrologic and temperature variables represent summer means, as these generally showed the strongest relationships with CAR; relationships with annual and growing season means were qualitatively similar but weaker. Relative (Rel) sediment load is represented by sed_{wet}.

From a climate-forcing perspective, the contrast between reference and disturbed sites highlights the long-term cost of diking, while the higher CAR in restored sites demonstrates the potential for tidal wetland restoration to deliver near-immediate carbon burial benefits, even as longer-term trajectories toward reference conditions continue to develop.

Restored marshes often had high CAR despite relatively low carbon density, underscoring our finding that accretion, and not carbon density, is the primary driver of CAR in PNW tidal wetlands. The low carbon density in restored sites may be due to organic matter dilution by mineral sediment inputs, especially in very young sites with high accretion rates (Drexler et al., 2019; McCarty et al., 2009; Poppe & Rybczyk, 2021; Wollenberg et al., 2018), which is supported by our negative correlation between carbon density and accretion rate (Figure S4 in Supporting Information S1). Elevated accretion and CAR in restored marshes have been widely reported in the PNW (Crooks et al., 2014; Davis et al., 2024; Drexler et al., 2019; Poppe & Rybczyk, 2021), indicating that sediment supply in PNW estuaries is sufficient to allow recovery from subsidence following diking and drainage. Such responses are not universal, likely reflecting sediment supply limitation (Giosan et al., 2014) or slower vegetation-driven soil development in organogenic marshes (Eagle et al., 2022). Even where rapid recovery occurs, however, high accretion rates are expected to be temporary. The restored marshes in this study are transitional systems of young to moderate age (1–27 years post restoration); therefore, we expect their accretion rates and CAR to decline as their elevation deficit is filled (Burden et al., 2019).

Disturbed sites had relatively low mean CAR but rates were also quite variable, particularly within dry pasture sites. Some of these sites were tilled, and these had the lowest (even negative) CAR values, while some untilled dry pastures had moderate CAR values as a result of accumulation of both above- and below-ground plant material. These sites had moderate carbon density but still relatively low accretion rates presumably due to lack of mineral sediment supply.

4.2. Timescale Dependence of CAR

Carbon accumulation rates in this study were strongly dependent on measurement timescale, with short-term CAR often exceeding long-term rates, but also showing weak correspondence with long-term values. This decoupling indicates that high recent CAR does not always translate to high long-term CAR, perhaps due to either changes in environmental conditions over time, or differences in the processes captured by short- and long-term estimates. Long-term CAR integrates variability in accretion and carbon density over a century of sediment deposition, compaction, and organic matter decomposition. On the other hand, short-term CAR may be more influenced by interannual variation in flooding, sediment supply, plant productivity, or other factors (Breithaupt et al., 2018). Nevertheless, short-term estimates of CAR are particularly useful for interpreting environmental controls, and for understanding the impacts of wetland restoration, disturbance, or hydrologic change.

4.3. PNW Values in a Global Context

Our estimates of CAR varied widely within some wetland types, making regional and global comparisons important for context. Because most published values represent long-term accumulation, the comparisons below focus primarily on long-term values. Mean long-term CAR for reference marshes in this study was slightly higher than the mean rate for several Oregon estuaries (Peck et al., 2020), and lower than means for individual estuaries in the Salish Sea (Crooks et al., 2014; Drexler et al., 2019; Poppe & Rybczyk, 2021; Table 2). Our reference marsh mean is similar to the global mean for temperate tidal marshes (IPCC, 2014), but lower than several other global marsh means (Mason et al., 2023; Ouyang & Lee, 2014; Wang et al., 2021). Two of those global syntheses included both short-term and long-term values in the CAR calculations, which may partially explain why their means are higher than our long-term values, but these means are higher than our short-term CAR as well. It is common to find a large range of values within this wetland type, however. Reference marsh CAR from this study

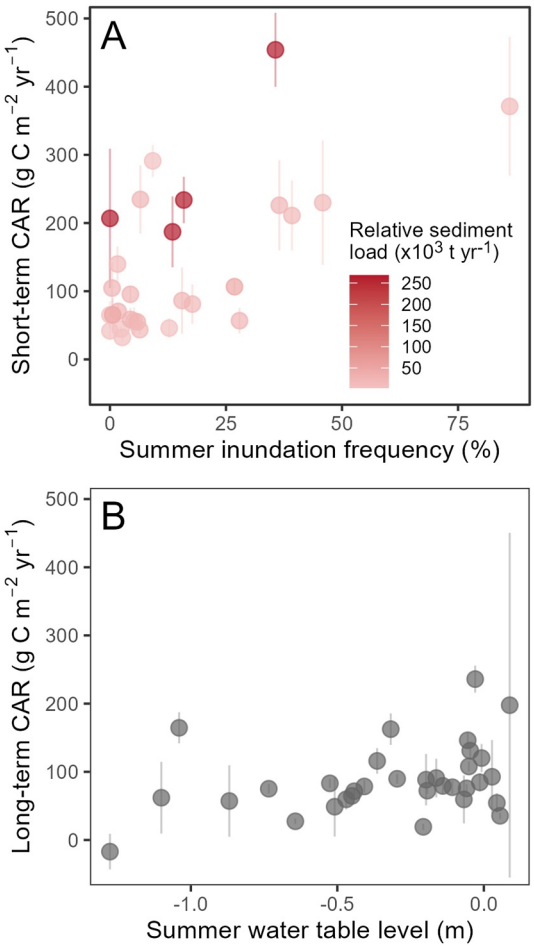

Figure 6. Relationships between carbon accumulation rate (CAR) and predictors included in the optimal models for (a) short-term and (b) long-term CAR. Error bars represent standard error.

ranged from 19 to 218 g C m^{-2} yr^{-1}, similar to other PNW studies (Drexler et al., 2019; Peck et al., 2020; Poppe & Rybczyk, 2021).

The restored marsh long-term CAR values we measured were generally higher than reference marshes but also more variable (Figure 4 and Table 2). This variability likely reflects the transitional nature of restored sites, which span a range of ages and hydrologic conditions as they continue to evolve after restoration. Our restored marsh CAR range is similar to the range reported by Drexler et al. (2019) at a relatively young restoration site in the Nisqually River Estuary, and the range reported in the Stillaguamish River Estuary (Poppe & Rybczyk, 2021). However, our restored site mean is lower than the global restored marsh mean, which is approximately double the global reference marsh mean from that study (Mason et al., 2023). Because the global restored marsh value combined both short- and long-term rates, direct comparisons to our long-term rates are imperfect. Even so, their global mean exceeds both our short- and long-term CAR.

There are few CAR measurements from non-mangrove tidal forested swamps globally (Friess et al., 2026). Although mangrove carbon dynamics are now well studied, non-mangrove tidal forests differ structurally and environmentally, particularly with regard to cold and salinity tolerance, understory cover, and elevation within the tidal frame (Friess et al., 2026). The Sitka spruce (*P. sitchensis*) tidal swamps included in this study are unique to the PNW, and although they were once common across the region, they are now rare (Brophy, 2025). While their CAR values are comparable with marshes, their carbon stocks (both soil carbon stocks and total ecosystem carbon stocks) are notably higher (Janousek, Krause, et al., 2025; Kauffman et al., 2020). Our mean long-term tidal swamp CAR was nearly identical to our reference marsh mean, and similar to values reported from other non-mangrove tidal forest ecosystems, including swamps in Georgia and South Carolina (Craft, 2012; Noe et al., 2016; Table 2). Global mean long-term CAR for mangroves tends to be higher than these non-mangrove values (Breithaupt & Steinmuller, 2022; Pérez et al., 2018), perhaps due to the lower elevation typical of many mangrove systems (Friess et al., 2026).

Estimates of CAR from nontidal pastures are similarly scarce, emphasizing the importance of this study in providing CAR values for these ecosystems. Although nontidal sites in the PNW had lower mean CAR than reference and restored marshes, others have found the opposite to be true. For example, diked former tidal wetlands in the Snohomish River Estuary in Washington had a wider range of CAR values, with some of these being higher than rates in reference and restored marsh and tidal swamp (Poppe & Rybczyk, 2022; Table 2). Brophy et al. (2017, 2018) reported similar means between diked and reference sites in Oregon. It is likely that highly variable post-disturbance management histories and hydrology is causing the high variability in CAR among these wetlands. Further study of nontidal pastures would allow us to better understand the site conditions driving this variability.

4.4. CAR Predictors

The wide range of CAR values observed in this and other studies in estuarine wetlands underscores the need to understand the geophysical and ecological drivers of CAR. We found that CAR values were more strongly influenced by sediment accretion rates than by soil carbon density in PNW estuaries, a pattern consistent with previous studies (Chmura et al., 2003; Peck et al., 2020; Wollenberg et al., 2018). In fact, accretion rates and carbon density were negatively related in our study. This negative correlation is likely the result of mineral sediments diluting organic matter when sedimentation rates are high, but may be also related to differences in decomposition following deposition. The strong relationship between accretion and CAR implies that as accretion rates increase in response to accelerating sea-level rise with sufficient sediment supply, CAR is likely to increase

Table 2
Comparison of Carbon Accumulation Rates (CAR) From This Study With Other Pacific Northwest US (PNW) and Global Values

Wetland type	Geographic region	Source	CAR mean ± SD (g C m^{-2} yr^{-1})	CAR range (g C m^{-2} yr^{-1})	N	Timescale	Notes
Reference tidal marsh	PNW (WA, OR)	This study	121 ± 74	44–235	12	Short-term	
			95 ± 47	19–218	24	Long-term	
	PNW (OR)	Peck et al. (2020)	77 ± 35		43	Long-term	High marsh only
	PNW (Nisqually Estuary, WA)	Drexler et al. (2019)	134 ± 19	115–168	6	Long-term	
	PNW (Stillaguamish Estuary, WA)	Poppe and Rybczyk (2021)	123 ± 86	37–283	8	Long-term	
	PNW (Snohomish Estuary, WA)	Crooks et al. (2014), Poppe and Rybczyk (2022)	120	NA	1	Long-term	
	PNW (Columbia Estuary, OR)	Brophy et al. (2017)	79 ± 36	45–130	5	Long-term	
	PNW (Tillamook Estuary, OR)	Brophy et al. (2018)	77 ± 11	69–90	3	Long-term	High marsh only
	Temperate global	IPCC (2014)	91 ± 19	5–465	66	Long-term	
	Global	Wang et al. (2021)	168 ± 7	1–1167	613	Long-term	
	Global	Ouyang and Lee (2014)	245 ± 26	18–1713	134	Short-term and long-term	
	Global	Mason et al. (2023)	213 ± 449	0–6123	312	Short-term and long-term	
Restored tidal marsh	PNW (WA, OR)	This study	218 ± 152	55–454	8	Short-term	
			106 ± 69	27–236	13	Long-term	
	PNW (Nisqually Estuary, WA)	Drexler et al. (2019)	164 ± 54	81–224	6	Long-term	
	PNW (Stillaguamish Estuary, WA)	Poppe and Rybczyk (2021)	230 ± 93	124–350	4	Long-term	
	Global	Mason et al. (2023)	441 ± 591	0–3660	82	Short-term and long-term	
Forested tidal swamp	PNW (WA, OR)	This study	110 ± 68	32–207	5	Short-term	Non-mangrove
			97 ± 35	60–163	11	Long-term	
	PNW (Snohomish Estuary, WA)	Crooks et al. (2014), Poppe and Rybczyk (2022)	101 ± 63	56–146	2	Long-term	Non-mangrove
	Georgia, USA	Craft (2012)	93 ± 5[a]		8	Long-term	Non-mangrove
	South Carolina, USA	Noe et al. (2016)	61 ± 28	8–121	19	Long-term	Non-mangrove
	Global	Breithaupt and Steinmuller (2022)	139 (+20/−18)[b]	2–1749	205	Long-term	Mangrove
	Global	Pérez et al. (2018)	173 ± 50	83–270	17	Long-term	Mangrove; least-disturbed sites only
Disturbed nontidal pasture	PNW (WA, OR)	This study	50 ± 13	42–65	3	Short-term	
			58 ± 54	−17–164	11	Long-term	
	PNW (Snohomish Estuary, WA)	Poppe and Rybczyk (2022), Crooks et al. (2014)	183 ± 171	62–304	2	Long-term	
	PNW (Columbia Estuary, OR)	Brophy et al. (2017)	80 ± 16	68–91	2	Long-term	
	PNW (Tillamook Estuary, OR)	Brophy et al. (2018)	150 ± 77	44–220	4	Long-term	

Note. Because long-term rates dominate the literature, comparisons focus on long-term values, however we include our short-term rates as some published syntheses combine both short- and long-term values. Short-term rates represent a sub-decadal measurement timescale; long-term rates represent decadal to centennial timescales, typically centennial-scale except at restored sites. N indicates the number of independent measurements contributing to each mean, and varies by timescale (i.e., soil cores for long-term estimates and site-level values for short-term estimates). Where studies reported combined means for multiple wetland or land-use types, we recalculated means from the available data and note our more limited groupings in the Notes column. [a]Standard error is reported; standard deviation was not available. [b]Geometric mean and 95% confidence intervals are reported, differing from the more common arithmetic mean ± SD.

as well, reinforcing the important reciprocal relationship between carbon sequestration and sea-level rise resilience in coastal restoration, among numerous other co-benefits (e.g., Familkhalili et al., 2023).

Short-term CAR was fairly well predicted by short-term, contemporary ecosystem predictors, with most predictors representing recent (1 year) conditions, similar to the CAR measurements. In contrast, long-term CAR was poorly predicted by these short-term variables. This is an important finding because long-term CAR is the metric most often used in blue carbon accounting, despite limited information on historical ecological conditions. Site hydrology was the best predictor of both long- and short-term CAR, but the weaker performance of the long-term model suggests that long-term CAR may be better represented by regional wetland-type averages than by site-level predictions. The poor explanatory power of the long-term CAR model may merely reflect the mismatch in both timescale and time period between predictor and response measurements, as environmental conditions including elevation, salinity, and sediment loads have likely changed over the past century. Alternatively, our predictor set may be overly focused on material delivery processes, perhaps missing variables related to the retention and preservation of sediment carbon, which may exert stronger control over CAR at longer timescales (Breithaupt et al., 2018). Finally, although our models included all land-use types together, carbon accumulation processes in disturbed sites may differ fundamentally from those in tidal wetlands, but our sample size was too limited to model land-use types independently.

Inundation frequency was positively correlated with short-term CAR, consistent with its role in delivering mineral sediments to tidal wetlands (Palinkas & Engelhardt, 2019). An alternative possible effect of inundation on CAR is the suppression of decomposition, which would increase soil carbon density. However, CAR was not correlated with carbon density in this study, suggesting that sediment delivery, rather than organic matter preservation, was the dominant process. Given the correlation between CAR and inundation frequency, we might also expect tidal elevation to be a strong predictor, since elevation is often used as a proxy for inundation, and the literature indicates that elevation is important for both carbon stocks (Janousek, Krause, et al., 2025) and accretion rates (French, 1993; Kirwan et al., 2010; Thorne et al., 2024). However, elevation has a positive relationship with carbon density and a negative relationship with accretion, weakening its overall effect when both are combined to calculate CAR. Perhaps more importantly, the muted effect of elevation on CAR may reflect its inconsistent ability to represent inundation across a diversity of sites.

Tidal elevation can serve as a reasonable proxy for inundation frequency in the context of a single land-use type and hydrogeomorphic setting, but it is less useful when considering multiple land uses and HGM settings. In hydrologically altered tidal wetlands, elevation is often decoupled from inundation due to dikes or channels limiting unimpeded tidal exchange. Disturbed sites in this study lacked any relationship between tidal elevation and inundation, because tidal influence has been intentionally restricted. Additionally, restored sites often have fewer tidal channel outlets when restored by dike breaching (Chamberlin et al., 2025; Hood, 2014), which can slow drainage and maintain flood conditions longer than would be predicted by elevation. Limiting the analysis to tidal sites results in a clearer relationship between elevation and inundation, although its strength varies by hydrogeomorphic setting, declining with river influence (Figure S7 in Supporting Information S1).

Relative sediment load (sed_{wet}) was the second most important predictor of short-term CAR, reinforcing the idea that carbon accumulation in minerogenic tidal wetlands depends on both sediment supply (watershed sediment loads) and delivery (inundation). In wetlands where sediment loads are high, even infrequent flooding can sustain high CAR, partially offsetting changes due to altered hydroperiods. Among the various sediment loading variables we considered, sed_{wet} represents the amount of sediment available per unit tidal wetland area, and its association with short-term CAR suggests that sediment trapping efficiency is high enough for sediment supply to influence CAR. Although sed_{wet} was not important to long-term CAR, others have found it to be an important control on long-term rates in reference marshes (Peck et al., 2020), suggesting that its influence may be more detectable within a single wetland type.

Water table level was more important to long-term CAR than inundation frequency, perhaps because it incorporates both belowground soil saturation and surface flooding. While inundation frequency represents the opportunity for sediment delivery, soil saturation can enhance the preservation of carbon through development of anoxic conditions that lead to reduced decomposition (Chapman et al., 2019), a process that likely plays a larger role in CAR over longer timescales. In short-term decomposition experiments in tidal wetlands, inundation effects on decomposition rates are weak or inconclusive (Janousek et al., 2017; Kirwan et al., 2013; Mueller et al., 2016),

and more research on the effects of varying hydrology and soil saturation on long-term carbon preservation is needed.

RSLR did not emerge as an important predictor of CAR in our models, despite mixed evidence for its role as a driver of accretion and CAR in other studies (e.g., Kirwan & Mudd, 2012; McTigue et al., 2019; Miller et al., 2022; Peck et al., 2020; Rogers et al., 2019; Wang et al., 2019, 2021; Weston et al., 2023; Yan et al., 2025). The RSLR values in this study ranged from 0.25 to 2.52 mm yr^{-1}, so the lack of effect is not likely due to lack of variability. It is possible that confounding of RSLR and sediment supply limited our ability to detect an independent effect of RSLR; across the PNW, higher RSLR occurs in the Salish Sea, where sediment loads are also relatively high. In addition, not all hydrogeomorphic settings are equally sensitive to tidal forcing; systems with stronger river influence may be less directly coupled to changes in sea level. A similar issue likely applies to latitude, which has been linked to CAR in global marsh and mangrove syntheses (Ouyang & Lee, 2014; Rosentreter et al., 2018). Latitude likely acts as a proxy for climate gradients, but in our study it covaried with other predictors such as sediment load.

4.5. Management Implications

Our results indicate a clear benefit of restoring former tidal wetlands to tidal influence to enhance both short- and long-term soil carbon accumulation. The mean restored marsh long-term CAR was 106 ± 69 g C m^{-2} yr^{-1}, which is nearly double the long-term mean for disturbed sites (58 ± 54 g C m^{-2} yr^{-1}). The restoration benefit is not simply an artifact of shorter measurement timeframes at those sites; short-term CAR (measured over 1 year across all sites) was also much higher at restored sites (218 ± 152 g C m^{-2} yr^{-1}) compared to disturbed sites (50 ± 13 g C m^{-2} yr^{-1}). The restored marshes studied here are generally young (1–27 years) and likely still recovering from subsidence, so we expect their rates to decline over time (Rowland et al., 2024). Even so, the mean long-term CAR in reference marshes (95 ± 47 g C m^{-2} yr^{-1}) was only somewhat lower than in restored marshes, suggesting that if or when restored marsh CAR declines to resemble reference rates, they will still be well above rates at disturbed sites. Given the apparent importance of inundation frequency for sediment delivery, restoring tidal hydrology to former tidal wetlands appears to be the most effective way to increase carbon sequestration in minerogenic tidal wetlands such as those in the PNW. Finally, while increasing water levels can lead to greater CAR, water level is also an important driver of methane emissions in the PNW (Schultz et al., 2023; Williams et al., 2025), so both effects need to be considered together when evaluating restoration as a natural climate solution.

Restoration wetland performance is often evaluated by comparing them to reference sites. However, few studies investigate blue carbon dynamics in actively disturbed sites to provide baseline data. In this study, we found that disturbed sites had the lowest CAR values, highlighting the need to include them in climate mitigation assessments to determine the added carbon accumulation benefits of restoration. However, measuring CAR in disturbed wetlands proved challenging; ^{210}Pb profiles were often mixed or at non-steady-state, and short-term marker horizons were difficult to interpret. SETs were often the only reliable method for detecting both accretion and subsidence. Further methodological work is needed to improve carbon accumulation estimates in disturbed tidal wetlands and help fill this data gap.

4.6. Methods Considerations

SETs provide measurements of net elevation change that integrate accretion together with shallow subsidence or expansion processes. In our PNW data sets, SET-derived elevation change rates were approximately four times higher than spatially-coupled long-term accretion rates derived from ^{210}Pb. Previous studies have used SET elevation change as a direct proxy for accretion in calculating CAR (Howe et al., 2009; Lovelock et al., 2014; Noyce et al., 2023; Rogers et al., 2013), but our evidence suggests that this equivalence is not universal. We applied a regionally derived conversion formula to improve comparability between the two methods, but this formula may not be transferable to other regions without further calibration, as differences between short- and long-term rates can be location-specific (Breithaupt et al., 2018). Globally, SET rates are more often lower than or equivalent to ^{210}Pb rates (Cahoon, 2024). When SET rates are higher, this is typically attributed to soil expansion from root production in wetlands with low mineral sediment inputs (Cahoon, 2024), a mechanism, that is, less likely in the predominantly minerogenic wetlands studied here. The most plausible explanation may be the measurement timeframe mismatch, with current rates of accretion being higher than historical rates due to

changes in site hydrology or sediment load over time. Feldspar accretion rates were similar to SET elevation change rates at the few sites where both were measured, lending support to this hypothesis. Parkinson et al. (2017) reported SET rates being four times higher than ^{210}Pb rates across Gulf of Mexico and east coast US marshes, which is similar to our findings, so although our rate discrepancy between methods is large, it is not unprecedented.

Another useful method for determining accretion rates in restored sites involves identifying a restoration marker layer based on an obvious shift in the soil bulk density profile (Arias-Ortiz et al., 2021; Drexler et al., 2019; Fitch et al., 2022), but we could only confidently identify such a layer in some of our restored site cores, and this approach does not work for sites still actively disturbed. Feldspar accretion rates were also difficult to interpret in many disturbed sites, particularly where reed canary grass (*Phalaris arundinacea*) roots redistributed the marker layer. Additionally, not all restored sites had SET infrastructure available to use adjusted accretion estimates, so some long-term rates were calculated directly from ^{210}Pb chronologies above the restoration horizon, representing intermediate timescales between SET elevation change rates and centennial-scale ^{210}Pb accretion rates. Importantly, only surface elevation change measurements (such as SET-based monitoring) can detect elevation loss, a process more likely to occur at disturbed sites. As a result, elevation change measurements may be the most reliable approach for quantifying vertical change within this land-use type.

4.7. Future Directions

Although this study expands available CAR data for different land-use types in estuarine wetlands, more estimates of CAR are needed from the less-studied wetland types, such as the Sitka spruce tidal forested swamps and the disturbed pasture sites, to better explain variability within these categories and enable modeling of wetland types separately. This might allow for a greater understanding of the impacts of management activity (e.g., cultivated vs. fallow) on blue carbon function, and could help us understand which baseline conditions are most conducive to impactful climate change mitigation upon restoration. Although we found hydrologic metrics such as inundation frequency and water table level to be the best predictors of CAR across sites and timescales, future work could consider additional environmental variables that might help explain more of the CAR variability, such as site-level sediment loads, water velocity, storm exposure, and plant stem density. Restored marsh CAR was most variable, and perhaps this variability could be better understood through further study of tidal channel morphology and drainage patterns within sites.

5. Conclusions

Across a broad range of estuarine wetland types, we found that CAR varied strongly by land use and measurement timescale. The weak relationship between short-term and long-term CAR indicates that recent carbon accumulation rates do not necessarily scale to long-term accumulation, highlighting the need to consider timescale in blue carbon estimates. Contemporary inundation frequency and relative sediment load explained much of the variation in short-term CAR, but provided limited insight into longer-term rates, pointing to the influence of historical conditions and longer-term carbon retention processes on centennial-scale CAR. Because hydrologic variables were the most important predictors across sites, routine monitoring of water levels could improve blue carbon assessments. While other variables such as elevation and RSLR are often strong predictors of accretion, they were not significant predictors of CAR in this study, likely due to the diversity of management histories and wetland types analyzed here. This highlights the importance of considering land-use history when applying generalized relationships to regional or global models.

CAR was lowest in nontidal pastures and highest in restored marshes, even very young restored sites. These results demonstrate the value of restoring tidal wetlands as natural climate solutions for quickly removing and storing atmospheric carbon dioxide. This regional analysis is unique in including a relatively wide range of wetland types, particularly tidal forested swamps and diked pastures that are both underrepresented in the literature. We also demonstrate a novel approach to determining ^{210}Pb-equivalent accretion rates in disturbed soils, using a combination of ^{210}Pb dating and SETs.

Conflict of Interest

The authors declare no conflicts of interest relevant to this study.

Availability Statement

Soil depth series data and metadata are available in the Smithsonian Environmental Research Center's repository at https://doi.org/10.25573/serc.27156465.v1 (Poppe et al., 2024). Analytical code is available at https://github.com/katrinapoppe/PNW_CAR.

Acknowledgments
This research is a product of the Pacific Northwest Blue Carbon Working Group and was funded by the Effects of Sea Level Rise program at NOAA-NCCOS (Grant NA19NOS4780176) and the National Estuarine Research Reserve System's Science Collaborative program (Grant NA19NOS4190058). KLP also received funding from an NSERC Discovery Grant to SHK. We thank the many landowners and managers who allowed access to study sites, including the Washington Department of Fish and Wildlife, Washington Department of Natural Resources, Snohomish County, Columbia Land Trust, North Coast Land Conservancy, South Slough NERR, Padilla Bay NERR, National Park Service, Port of Astoria, City of Coos Bay, Warrenton Public Works, and private landowners. We are grateful to the Washington Department of Fish and Wildlife for allowing us to use their SET data, and to the Institute for Applied Ecology and US EPA for loaning data loggers. We thank Ian Rodger, Finn Tobias, Rachel Yonemura, and Thomas A. Lloyd for providing field and lab assistance. We thank the anonymous reviewers and editors for their comments and suggestions, which improved the manuscript.

References

Adame, M. F., Neil, D., Wright, S. F., & Lovelock, C. E. (2010). Sedimentation within and among mangrove forests along a gradient of geomorphological settings. *Estuarine, Coastal and Shelf Science*, *86*(1), 21–30. https://doi.org/10.1016/j.ecss.2009.10.013

Arias-Ortiz, A., Masqué, P., Garcia-Orellana, J., Serrano, O., Mazarrasa, I., Marbá, N., et al. (2018). Reviews and syntheses: ^{210}Pb-derived sediment and carbon accumulation rates in vegetated coastal ecosystems—Setting the record straight. *Biogeosciences*, *15*(22), 6791–6818. https://doi.org/10.5194/bg-15-6791-2018

Arias-Ortiz, A., Oikawa, P. Y., Carlin, J., Masqué, P., Shahan, J., Kanneg, S., et al. (2021). Tidal and nontidal marsh restoration: A trade-off between carbon sequestration, methane emissions, and soil accretion. *JGR Biogeosciences*, *126*(12), e2021JG006573. https://doi.org/10.1029/2021JG006573

Bartoń, K. (2023). MuMIn: Multi-model inference: R package (version 1.47.5) [Software]. *Institute for Statistics and Mathematics*. Retrieved from https://CRAN.R-project.org/package=MuMIn

Bates, D., Machler, M., Bolker, B., & Walker, S. (2015). Fitting linear mixed-effects models using lme4. *Journal of Statistical Software*, *67*(1), 1–48. https://doi.org/10.18637/jss.v067.i01

Breithaupt, J. L., Smoak, J. M., Byrne, R. H., Waters, M. N., Moyer, R. P., & Sanders, C. J. (2018). Avoiding timescale bias in assessments of coastal wetland vertical change. *Limnology and Oceanography*, *63*(S1), S477–S495. https://doi.org/10.1002/lno.10783

Breithaupt, J. L., & Steinmuller, H. E. (2022). Refining the global estimate of mangrove carbon burial rates using sedimentary and geomorphic settings. *Geophysical Research Letters*, *49*(18), e2022GL100177. https://doi.org/10.1029/2022GL100177

Brophy, L. S. (2025). Where have all the tidal forests gone? Mapping losses of forested and emergent tidal wetlands on the Oregon coast, USA. *Estuarine, Coastal and Shelf Science*, *328*, 109542. https://doi.org/10.1016/j.ecss.2025.109542

Brophy, L. S., Brown, L. A., Ewald, M. J., & Peck, E. K. (2017). *Baseline monitoring at Wallooskee-Youngs restoration site, 2015, Part 2: Blue carbon, ecosystem drivers, and biotic responses*. Report prepared for U.S. Fish and Wildlife Service, Portland, Oregon. Corvallis, Oregon, USA. Institute for Applied Ecology. https://doi.org/10.13140/RG.2.2.20203.77609

Brophy, L. S., Greene, C. M., Hare, V. C., Holycross, B., Lanier, A., Heady, W. N., et al. (2019). Insights into estuary habitat loss in the western United States using a new method for mapping maximum extent of tidal wetlands. *PLoS One*, *14*(8), e0218558. https://doi.org/10.1371/journal.pone.0218558

Brophy, L. S., Peck, E. K., Bailey, S. J., Cornu, C. E., Wheatcroft, R. A., Brown, L. A., & Ewald, M. J. (2018). *Southern Flow Corridor effectiveness monitoring, 2015-2017: Sediment accretion and blue carbon*. Report prepared for Tillamook County and the Tillamook Estuaries Partnership, Tillamook, Oregon, USA. Institute for Applied Ecology. https://doi.org/10.13140/RG.2.2.28592.38405

Burden, A., Garbutt, R. A., Evans, C. D., Jones, D. L., & Cooper, D. M. (2019). Effect of restoration on saltmarsh carbon accumulation in eastern England. *Biology Letters*, *15*(1), 20180773. https://doi.org/10.1098/rsbl.2018.0773

Cahoon, D. R. (2024). Measuring and interpreting the surface and shallow subsurface process influences on coastal wetland elevation: A review. *Estuaries and Coasts*, *47*(7), 1708–1734. https://doi.org/10.1007/s12237-024-01332-z

Chamberlin, J. W., Stefankiv, O., Beamer, E. M., Greene, C. M., Hood, W. G., & Munsch, S. H. (2025). Estimating estuary habitat change and functional trajectory of restoration projects over two decades in Puget Sound, WA. *Frontiers in Marine Science*, *12*, 1549344. https://doi.org/10.3389/fmars.2025.1549344

Chapin, F. S., Matson, P. A., & Vitousek, P. M. (2011). *Principles of terrestrial ecosystem ecology* (2nd ed.). Springer.

Chapin, F. S., Woodwell, G. M., Randerson, J. T., Rastetter, E. B., Lovett, G. M., Baldocchi, D. D., et al. (2006). Reconciling carbon-cycle concepts, terminology, and methods. *Ecosystems*, *9*(7), 1041–1050. https://doi.org/10.1007/s10021-005-0105-7

Chapman, S. K., Hayes, M. A., Kelly, B., & Langley, J. A. (2019). Exploring the oxygen sensitivity of wetland soil carbon mineralization. *Biology Letters*, *15*(1), 20180407. https://doi.org/10.1098/rsbl.2018.0407

Chmura, G. L., Anisfeld, S. C., Cahoon, D. R., & Lynch, J. C. (2003). Global carbon sequestration in tidal, saline wetland soils. *Global Biogeochemical Cycles*, *17*(4), 1111. https://doi.org/10.1029/2002GB001917

Chmura, G. L., & Hung, G. A. (2004). Controls on salt marsh accretion: A test in salt marshes of Eastern Canada. *Estuaries*, *27*(1), 70–81. https://doi.org/10.1007/BF02803561

Craft, C. (2012). Tidal freshwater forest accretion does not keep pace with sea level rise. *Global Change Biology*, *18*(12), 3615–3623. https://doi.org/10.1111/gcb.12009

Crooks, S., Beers, L., Settelmyer, S., Swails, E., Emmett-Mattox, S., & Cornu, C. (2020). *Scoping assessment for Pacific Northwest blue carbon finance projects*. Silvestrum Climate Associates.

Crooks, S., Rybczyk, J., O'Connell, K., Devier, D. L., Poppe, K., & Emmett-Mattox, S. (2014). *Coastal blue carbon opportunity assessment for the Snohomish Estuary: The climate benefits of estuary restoration*. Report prepared for Restore America's Estuaries, Arlington, VA. Seattle, WA: Environmental Science Associates; Bellingham, WA: Western Washington University; Seattle, WA: EarthCorps; Arlington, VA. Restore America's Estuaries.

Davis, M. J., Poppe, K. L., Rybczyk, J. M., Grossman, E. E., Woo, I., Chamberlin, J. W., et al. (2024). Vulnerability to sea-level rise varies among estuaries and habitat types: Lessons learned from a network of surface elevation tables in Puget Sound. *Estuaries and Coasts*, *47*(7), 1918–1940. https://doi.org/10.1007/s12237-024-01335-w

Drexler, J. Z., Woo, I., Fuller, C. C., & Nakai, G. (2019). Carbon accumulation and vertical accretion in a restored versus historic salt marsh in southern Puget Sound, Washington, United States. *Restoration Ecology*, *27*(5), 1117–1127. https://doi.org/10.1111/rec.12941

Eagle, M. J., Kroeger, K. D., Spivak, A. C., Wang, F., Tang, J., Abdul-Aziz, et al. (2022). Soil carbon consequences of historic hydrologic impairment and recent restoration in coastal wetlands. *Science of the Total Environment*, *848*, 157682. https://doi.org/10.1016/j.scitotenv.2022.157682

Familkhalili, R., Davis, J., Currin, C. A., Heppe, M. E., & Cohen, S. (2023). Quantifying the benefits of wetland restoration under projected sea level rise. *Frontiers in Marine Science*, *10*, 1187276. https://doi.org/10.3389/fmars.2023.1187276

Fennessy, M. S., Ibánez, C., Calvo-Cubero, J., Sharpe, P., Rovira, A., Callaway, J., & Caiola, N. (2019). Environmental controls on carbon sequestration, sediment accretion, and elevation change in the Ebro River Delta: Implications for wetland restoration. *Estuarine, Coastal and Shelf Science*, *222*, 32–42. https://doi.org/10.1016/j.ecss.2019.03.023

Fitch, A. A., Blount, K., Reynolds, I., & Bridgham, S. D. (2022). Partial recovery of microbial function in restored coastal marshes of Oregon, USA. *Soil Science of America Journal*, *86*(3), 831–846. https://doi.org/10.1002/saj2.20383

French, J. R. (1993). Numerical simulation of vertical marsh growth and adjustment to accelerated sea-level rise, North Norfolk, U.K. *Earth Surface Processes and Landforms*, *18*(1), 63–81. https://doi.org/10.1002/esp.3290180105

Friess, D. A., Adame, M. F., Kelleway, J. J., Krauss, K. W., & Noe, G. B. (2026). Tidal forested wetlands can be incorporated into blue carbon conservation and restoration strategies. *Current Forestry Reports*, *12*(1), 9. https://doi.org/10.1007/s40725-026-00271-1

Giosan, L., Syvitski, J., Constantinescu, S. D., & Day, J. (2014). Climate change: Protect the world's deltas. *Nature*, *516*(7529), 31–33. https://doi.org/10.1038/516031a

Heiri, O., Lotter, A. F., & Lemcke, G. (2001). Loss on ignition as a method for estimating organic and carbonate content in sediments: Reproducibility and comparability of results. *Journal of Paleolimnology*, *25*(1), 101–110. https://doi.org/10.1023/A:1008119611481

Holmquist, J. R., Windham-Myers, L., Bernal, B., Byrd, K. B., Crooks, S., Megonigal, J. P., et al. (2018). Uncertainty in United States coastal wetland greenhouse gas inventorying. *Environmental Research Letters*, *13*(11), 115005. https://doi.org/10.1088/1748-9326/aae157

Hood, W. G. (2014). Differences in tidal channel network geometry between reference marshes and marshes restored by historical dike breaching. *Ecological Engineering*, *71*, 563–573. https://doi.org/10.1016/j.ecoleng.2014.07.076

Hothorn, T., Hornik, K., van de Wiel, M. A., & Zeileis, A. (2006). A lego system for conditional inference. *The American Statistician*, *60*(3), 257–263. https://doi.org/10.1198/000313006X118430

Hothorn, T., & Zeileis, A. (2015). partykit: A modular toolkit for recursive partitioning in R. *Journal of Machine Learning Research*, *16*, 3905–3909. Retrieved from https://jmlr.org/papers/v16/hothorn15a.html

Howe, A. J., Rodriguez, J. F., & Saco, P. M. (2009). Surface evolution and carbon sequestration in disturbed and undisturbed wetland soils of the Hunter estuary, southeast Australia. *Estuarine, Coastal and Shelf Science*, *84*(1), 75–83. https://doi.org/10.1016/j.ecss.2009.06.006

IPCC. (2014). Coastal wetlands. In T. Hiraishi, T. Krug, K. Tanabe, N. Srivastava, J. Baasansuren, et al. (Eds.), *2013 supplement to the 2006 IPCC guidelines for national greenhouse gas inventories: Wetlands*. IPCC.

IPCC. (2019). Wetlands. In E. Calvo Buendia, K. Tanabe, A. Kranjc, J. Baasansuren, M. Fukuda, et al. (Eds.), *2019 refinement to the 2006 IPCC guidelines for national greenhouse gas inventories: Volume 4: Agriculture, forestry and other land use*. IPCC.

Janousek, C., & Cornu, C. (2025). Water levels in the Grays Harbor and Columbia River estuaries, Washington [Dataset]. *Knowledge Network for Biocomplexity*. https://doi.org/10.5063/F1TQ601V

Janousek, C., Cornu, C., & Williams, T. (2025). Water levels in the Skagit and Nisqually River estuaries, Washington [Dataset]. *Knowledge Network for Biocomplexity*. https://doi.org/10.5063/F17W69PJ

Janousek, C. N., Buffington, K., Guntenspergen, G., Thorne, K., Dugger, B., & Takekawa, T. (2017). Inundation, vegetation, and soil effects on litter decomposition in Pacific coast tidal marshes. *Ecosystems*, *20*(7), 1296–1310. https://doi.org/10.1007/s10021-017-0111-6

Janousek, C. N., Krause, J. R., Drexler, J. Z., Buffington, K. Z., Poppe, K. L., Peck, E., et al. (2025). Blue carbon stocks along the Pacific coast of North America are mainly driven by local rather than regional factors. *Global Biogeochemical Cycles*, *39*(3), e2024GB008239. https://doi.org/10.1029/2024GB008239

Kassambara, A. (2025). rstatix: Pipe-friendly framework for basic statistical tests. R package (Version 0.7.3) [Software]. *The Comprehensive R Archive Network*. Retrieved from https://CRAN.R-project.org/package=rstatix

Kauffman, J. B., Giovanonni, L., Kelly, J., Dunstan, N., Borde, A., Diefenderfer, H., et al. (2020). Total ecosystem carbon stocks at the marine-terrestrial interface: Blue carbon of the Pacific Northwest Coast, United States. *Global Change Biology*, *26*(10), 5679–5692. https://doi.org/10.1111/gcb.15248

Kirwan, M. L., Guntenspergen, G. R., D'Alpaos, A., Morris, J. T., Mudd, S. M., & Temmerman, S. (2010). Limits on the adaptability of coastal marshes to rising sea level. *Geophysical Research Letters*, *37*(23), L23401. https://doi.org/10.1029/2010GL045489

Kirwan, M. L., Langley, J. A., Guntenspergen, G. R., & Megonigal, J. P. (2013). The impact of sea-level rise on organic matter decay rates in Chesapeake Bay brackish tidal marshes. *Biogeosciences*, *10*(3), 1869–1876. https://doi.org/10.5194/bg-10-1869-2013

Kirwan, M. L., & Mudd, S. M. (2012). Response of salt-marsh carbon accumulation to climate change. *Nature*, *489*(7417), 550–553. https://doi.org/10.1038/nature11440

Lovelock, C. E., Adame, M. F., Bennion, V., Hayes, M., O'Mara, J., Reef, R., & Santini, N. S. (2014). Contemporary rates of carbon sequestration through vertical accretion of sediments in mangrove forests and saltmarshes of South East Queensland, Australia. *Estuaries and Coasts*, *37*(3), 763–771. https://doi.org/10.1007/s12237-013-9702-4

Lynch, J. C., Hensel, P., & Cahoon, D. R. (2015). *The surface elevation table and marker horizon technique: A protocol for monitoring wetland elevation dynamics*. (Report NPS/NCBN/NRR-2015/1078). National Park Service.

Macreadie, P. I., Anton, A., Raven, J. A., Beaumont, N., Connolly, R. M., Friess, D. A., et al. (2019). The future of blue carbon science. *Nature Communications*, *10*(1), 3998. https://doi.org/10.1038/s41467-019-11693-w

Macreadie, P. I., Costa, M. D. P., Atwood, T. B., Friess, D. A., Kelleway, J. J., Kennedy, H., et al. (2021). Blue carbon as a natural climate solution. *Nature Reviews Earth & Environment*, *2*(12), 826–839. https://doi.org/10.1038/s43017-021-00224-1

Mason, V. G., Burden, A., Epstein, G., Jupe, L. K., Wood, K. A., & Skov, M. W. (2023). Blue carbon benefits from global saltmarsh restoration. *Global Change Biology*, *29*(23), 6517–6545. https://doi.org/10.1111/gcb.16943

McCarty, G., Pachepsky, Y., & Ritchie, J. (2009). Impact of sedimentation on wetland carbon sequestration in an agricultural watershed. *Journal of Environmental Quality*, *38*(2), 804–813. https://doi.org/10.2134/jeq2008.0012

McLeod, E., Chmura, G. L., Bouillon, S., Salm, R., Björk, M., Duarte, C. M., et al. (2011). A blueprint for blue carbon: Toward an improved understanding of the role of vegetated coastal habitats in sequestering CO_2. *Frontiers in Ecology and the Environment*, *9*(10), 552–560. https://doi.org/10.1890/110004

McTigue, N., Davis, J., Rodriguez, A. B., McKee, B., Atencio, A., & Currin, C. (2019). Sea level rise explains changing carbon accumulation rates in a salt marsh over the past two millenia. *JGR Biogeosciences*, *124*(10), 2945–2957. https://doi.org/10.1029/2019JG005207

Miller, C. B., Rodriguez, A. B., Bost, M. C., McKee, B. A., & McTigue, N. D. (2022). Carbon accumulation rates are highest at young and expanding salt marsh edges. *Communications Earth & Environment*, *3*(1), 1–9. https://doi.org/10.1038/s43247-022-00501-x

Mueller, P., Jensen, K., & Megonigal, J. P. (2016). Plants mediate soil organic matter decomposition in response to sea level rise. *Global Change Biology*, *22*(1), 404–414. https://doi.org/10.1111/gcb.13082

NOAA. (2003). *Computational techniques for tidal datums handbook*. (NOAA Special Publication NOS CO-OPS 2). National Oceanic and Atmospheric Administration.

Noe, G. B., Hupp, C. R., Bernhardt, C. E., & Krauss, K. W. (2016). Contemporary deposition and long-term accumulation of sediment and nutrients by tidal freshwater forested wetlands impacted by sea level rise. *Estuaries and Coasts*, *39*(4), 1006–1019. https://doi.org/10.1007/s12237-016-0066-4

Noyce, G. L., Smith, A. J., Kirwan, M. L., Rich, R. L., & Megonigal, J. P. (2023). Oxygen priming induced by elevated CO_2 reduces carbon accumulation and methane emissions in coastal wetlands. *Nature Geoscience*, *16*(1), 63–68. https://doi.org/10.1038/s41561-022-01070-6

Ouyang, X., & Lee, S. Y. (2014). Updated estimates of carbon accumulation rates in coastal marsh sediments. *Biogeosciences*, *11*(18), 5057–5071. https://doi.org/10.5194/bg-11-5057-2014

Pacific Marine and Estuarine Fish Habitat Partnership. (2019). West Coast USA estuarine Biotic Habitat, V1.2. Retrieved from https://www.pacificfishhabitat.org/data/estuarine-biotic-habitat

Palinkas, C. M., & Engelhardt, K. A. M. (2019). Influence of inundation and suspended-sediment concentrations on spatiotemporal sedimentation patterns in a tidal freshwater marsh. *Wetlands and Climate Change*, *39*(3), 507–520. https://doi.org/10.1007/s13157-018-1097-3

Parkinson, R. W., Craft, C., DeLaune, R. D., Donoghue, J. F., Meeder, J. F., Morris, J., & Turner, R. (2017). Marsh vulnerability to sea-level rise. *Nature Climate Change*, *7*(11), 756. https://doi.org/10.1038/nclimate3424

Peck, E. K., Wheatcroft, R. A., & Brophy, L. S. (2020). Controls on sediment accretion and blue carbon burial in tidal saline wetlands: Insights from the Oregon coast, USA. *JGR Biogeosciences*, *125*(2), e2019JG005464. https://doi.org/10.1029/2019JG005464

Pérez, A., Libardoni, G. B., & Sanders, C. J. (2018). Factors influencing organic carbon accumulation in mangrove ecosystems. *Biology Letters*, *14*(10), 20180237. https://doi.org/10.1098/rsbl.2018.0237

Poppe, K., Bridgham, S. D., Janousek, C., Williams, T., Cornu, C., Perillat, H., et al. (2024). Soil carbon stocks and long-term accretion rates in tidal marshes, tidal swamps, and former tidal wetlands in eight estuaries in the Pacific Northwest, USA [Dataset]. *Smithsonian Environmental Research Center*. https://doi.org/10.25573/serc.27156465.v1

Poppe, K. L., & Rybczyk, J. M. (2021). Tidal marsh restoration enhances sediment accretion and carbon accumulation in the Stillaguamish River estuary, Washington. *PLoS One*, *16*(9), e0257244. https://doi.org/10.1371/journal.pone.0257244

Poppe, K. L., & Rybczyk, J. M. (2022). Sediment carbon stocks and sequestration rates in the Pacific Northwest region of Washington, USA [Dataset]. *Smithsonian Environmental Research Center*. https://doi.org/10.25573/serc.10005248.v2

R Core Team. (2025). *R: A language and environment for statistical computing*. R Foundation for Statistical Computing. Retrieved from https://www.R-project.org/

Robbins, J. A., Edgington, D. N., & Kemp, A. L. W. (1978). Comparative ^{210}Pb, ^{137}Cs, and pollen chronologies of sediments from Lake Ontario and Erie. *Quaternary Research*, *10*(2), 256–278. https://doi.org/10.1016/0033-5894(78)90105-9

Rogers, K., Kelleway, J. J., Saintilan, N., Megonigal, J. P., Adams, J. B., Holmquist, J. R., et al. (2019). Wetland carbon storage controlled by millennial-scale variation in relative sea-level rise. *Nature*, *567*(7746), 91–95. https://doi.org/10.1038/s41586-019-0951-7

Rogers, K., Saintilan, N., & Copeland, C. (2013). Managed retreat of saline coastal wetlands: Challenges and opportunities. *Estuaries and Coasts*, *37*(1), 67–78. https://doi.org/10.1007/s12237-013-9664-6

Rosentreter, J. A., Maher, D. T., Erler, D. V., Murray, R. H., & Eyre, B. D. (2018). Methane emissions partially offset "blue carbon" burial in mangroves. *Science Advances*, *4*(6), eaao4985. https://doi.org/10.1126/sciadv.aao4985

Rowland, P. I., Wartman, M., Bursic, J., & Carnell, P. (2024). Restored and created tidal marshes recover ecosystem services over time. *Environmental and Sustainability Indicators*, *24*, 100539. https://doi.org/10.1016/j.indic.2024.100539

Schultz, M. A., Janousek, C. N., Brophy, L. S., Schmitt, J., & Bridgham, S. D. (2023). How management interacts with environmental drivers to control greenhouse gas fluxes from Pacific Northwest coastal wetlands. *Biogeochemistry*, *165*(2), 165–190. https://doi.org/10.1007/s10533-023-01071-6

Swanson, K. M., Drexler, J. Z., Schoellhammer, D. H., Thorne, K. M., Casazza, M. L., Overton, C. T., et al. (2014). Wetland accretion rate model of ecosystem resilience (WARMER) and its application to habitat sustainability for endangered species in the San Francisco estuary. *Estuaries and Coasts*, *37*(2), 476–492. https://doi.org/10.1007/s12237-013-9694-0

Taillardat, P., Thompson, B. S., Garneau, M., Trottier, K., & Friess, D. A. (2020). Climate change mitigation potential of wetlands and the cost-effectiveness of their restoration. *Interface Focus*, *10*(5), 20190129. https://doi.org/10.1098/rsfs.2019.0129

Talke, S. A., Mahedy, A., Jay, D. A., Lau, P., Hilley, C., & Hudson, A. (2020). Sea level, tidal and river flow trends in the Lower Columbia River Estuary, 1853-present. *Journal of Geophysical Research: Oceans*, *125*(3), e2019JC015656. https://doi.org/10.1029/2019JC015656

Thorne, K. M., Bristow, M. L., Rankin, L. L., Kovalenko, K. E., Neville, J. A., Freeman, C. M., & Guntenspergen, G. R. (2024). Understanding marsh elevation and accretion processes and vulnerability to rising sea levels across climatic and geomorphic gradients in California, USA. *Estuaries and Coasts*, *47*(7), 1972–1992. https://doi.org/10.1007/s12237-023-01298-4

Wang, F., Lu, X., Sanders, C. J., & Tang, J. (2019). Tidal wetland resilience to sea level rise increases carbon sequestration capacity in United States. *Nature Communications*, *10*(1), 5434. https://doi.org/10.1038/s41467-019-13294-z

Wang, F., Sanders, C. J., Santos, I. R., Tang, J., Schurech, M., Kirwan, M. L., et al. (2021). Global blue carbon accumulation in tidal wetlands increases with climate change. *National Science Review*, *8*(9), nwaa296. https://doi.org/10.1093/nsr/nwaa296

Weston, N. B., Rodriguez, E., Donnelly, B., Solohin, E., Jezycki, K., Demberger, S., et al. (2023). Recent accumulation of wetland accretion and carbon accumulation along the U.S. East Coast. *Earth's Future*, *11*(3), e2022EF003037. https://doi.org/10.1029/2022EF003037

Williams, T., Janousek, C. N., McKeon, M. A., Diefenderfer, H. L., Cornu, C. E., Borde, A. B., et al. (2025). Methane and nitrous oxide fluxes from reference, restored, and disturbed estuarine wetlands in Pacific Northwest, USA. *Ecological Applications*, *35*(2), e70011. https://doi.org/10.1002/eap.70011

Wollenberg, J. T., Ollerhead, J., & Chmura, G. L. (2018). Rapid carbon accumulation following managed realignment on the Bay of Fundy. *PLoS One*, *13*(3), e0193930. https://doi.org/10.1371/journal.pone.0193930

Yan, S.-J., Hao, Q., Yan, Z., & Yang, R.-M. (2025). Global patterns and driving factors of the carbon accumulation rate in coastal wetlands. *Earth-Science Reviews*, *269*, 105199. https://doi.org/10.1016/j.earscirev.2025.105199

Zhang, D. (2024). rsq: R-squared and related measures. R package (version 2.7) [Software]. *The Comprehensive R Archive Network*. Retrieved from https://CRAN.R-project.org/package=rsq